

Annealing Effects on Orientation in Dynamically Sheared Diblock Copolymers

Yuanming Zhang, Ulrich Wiesner,* Yuliang Yang,[†] Tadeusz Pakula, and Hans W. Spiess

Max-Planck-Institut für Polymerforschung, Postfach 3148, D-55021 Mainz, Germany

Received January 27, 1996; Revised Manuscript Received April 29, 1996[®]

ABSTRACT: The frequency dependence of the lamellar orientation is investigated for a nearly symmetric polystyrene–polyisoprene diblock copolymer of low molecular weight under large-amplitude oscillatory shear near the order–disorder transition temperature (T_{ODT}). It is demonstrated that in the case of low frequencies not only the linear viscoelastic response but also the thermal history of the diblock copolymer must be known in order to predict the orientation behavior. For samples annealed at temperatures far below T_{ODT} but above the glass transition temperatures of both blocks, parallel alignment of the unit normal with respect to the velocity gradient direction is observed. For samples quenched from above T_{ODT} , preferential perpendicular alignment can be achieved. It is shown, however, that only for annealed samples uniform orientation with optimum order parameters is obtained.

Introduction

The application of large-amplitude mechanical fields to block copolymers in the melt state has attracted much interest in recent years.^{1–18} This is accompanied by an increasing appreciation of the remarkable diversity of such nonequilibrium phenomena in what is often called the emerging field of “soft matter” in general. Besides polymer melts and solutions, this field also includes materials such as liquid crystals, surfactants, or micro-emulsions.^{19,20} In such systems, because of their complexity, one is often far from a thorough theoretical understanding. Instead of testing specific predictions of theory, one seeks for the main mechanisms that govern the observed behavior.

This is particularly true for the flow alignment of lamellar diblock copolymers. Although a number of studies elucidated conditions for producing single crystal type morphologies with layer normals along different directions,^{4,21–28} the understanding of the underlying mechanisms is still relatively poor. In a first contribution, we have therefore investigated the effects of large-amplitude oscillatory shear flow on a lamellar polystyrene (PS)–polyisoprene (PI) diblock copolymer of low molecular weight.²⁹ For temperatures close to the order–disorder transition (T_{ODT}), we reported the existence of three frequency regimes for the orientational behavior related to the dynamic shear viscosity of the system. In these regimes, shear flow was leading to parallel, perpendicular, and parallel orientation, respectively, of the unit normal of the lamellae with respect to the velocity gradient direction of the flow field. In a subsequent publication,³⁰ we showed that for lamellar PS–PI diblock copolymers of intermediate molecular weights where the chain dynamics is significantly affected by topological constraints, i.e. entanglement couplings, the third principal orientation direction can be achieved at temperatures far below T_{ODT} . In this case, the unit normal of the lamellae is oriented parallel to the flow direction. Using concepts from the tube model of entangled polymer melts and characteristic features of the chain conformational statistics of diblock copolymers, we suggested a mechanism for the formation of this orientation component.

In both publications, we pointed out that for the understanding of the nonequilibrium phenomena in block copolymers under large-amplitude oscillatory shear flow, i.e. in the nonlinear regime, the coupling between external flow field and polymer dynamics is of fundamental importance. This coupling is mainly reflected in the time (or frequency) dependence of the *linear* viscoelastic properties of diblock copolymers. It was therefore suggested that, likewise in the *nonlinear* regime, the change in the time scale of the flow with respect to the characteristic time scales of the block copolymer dynamics would provide the key to understanding the orientation behavior of the phase-separated microstructure. From studies on block copolymers and other complex polymer fluids like polymeric liquid crystals, however, it is known that the thermal history of the sample often has significant effects on the observed behavior, in particular at temperatures close to phase transitions. In the present paper, we will therefore investigate the effect of annealing on the orientation behavior of a lamellar PS–PI diblock copolymer of low molecular weight at temperatures close to T_{ODT} . We show that, in order to predict the orientation behavior, one must know the linear viscoelastic response of the diblock *and* the thermal history of the sample.

Experimental Section

The lamellar poly(styrene-*b*-isoprene) diblock copolymer studied (termed PS–PI-7 in our nomenclature) was synthesized by anionic polymerization using cyclohexane as solvent and *sec*-butyllithium as initiator. The PS and PI block number-average molecular weights M_n are 9900 and 9100, respectively, as determined by GPC for the PS precursor and ¹³C NMR for the PI block. The dispersity M_w/M_n as determined by GPC for the block copolymer is 1.09. All GPC's were performed using polystyrene as standards. The uncertainties in the molecular weight determination are about 5% for both techniques. The T_g 's for the PS and PI blocks as determined by DSC with a heating rate of 10 K/min are 341 and 213 K, respectively. Comparing these values with those usually found for PS (378 K) and PI (213 K) homopolymers of sufficiently high molecular weight, it follows that the PS block component suffers a depression of T_g . This is a result of its low molecular weight and a possible plasticizing effect by the PI chains. It is important to notice at this point that the thermodynamics and consequently the dynamics of PS–PI block copolymers are extremely sensitive to changes in the molecular weight as evidenced for example by NMR measurements on this and related systems.^{31–33} T_{ODT} as determined by the temperature

* To whom correspondence should be addressed.

[†]Department of Macromolecular Science, Fudan University, Shanghai, 200433, P.R.C.

[®] Abstract published in *Advance ACS Abstracts*, June 15, 1996.

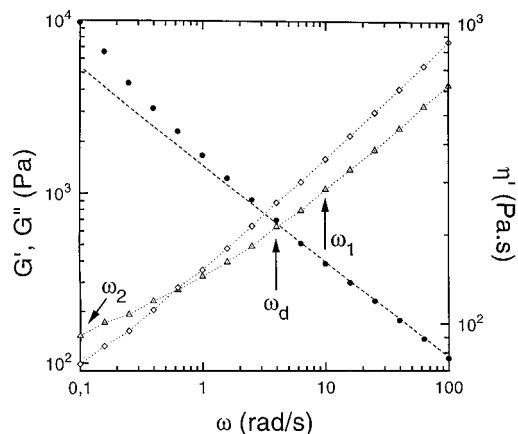


Figure 1. Dynamic shear moduli G' (Δ) and G'' (\diamond) and shear viscosity $\eta' = G''/\omega$ (\bullet) of PS-PI-7 at 409 K measured in parallel-plate geometry. Dotted lines through the moduli data points are guides for the eye. Indicated with an arrow is the critical frequency ω_d where the dynamic shear viscosity starts to deviate from the line of constant slope (---). Also indicated by arrows are the two frequencies $\omega_1 = 10$ rad/s and $\omega_2 = 0.1$ rad/s used in the large-amplitude oscillatory shear experiments described in the text.

dependence of the storage modulus $G'(T)^{34,35}$ at $\omega = 3$ rad/s is 424 ± 1 K. In all samples 2,6-di-*tert*-butyl-4-methylphenol was used as an antioxidant.

Samples were pressed at room temperature into disks with diameter of 25 mm and thickness of 1 mm and then thermally treated as described in the following section. A Rheometrics Model 800 (RMS-800) mechanical spectrometer was used in the parallel-plate geometry for the large-amplitude oscillatory shear experiments (100% strain if not stated otherwise) on these sample disks at different frequencies as well as for the dynamic mechanical measurements on the unoriented samples.

SAXS experiments were performed on specimens cut from shear-oriented sheets. A Rigaku Rotaflex X-ray source at 0.154 nm (Cu K α) was employed. A three-pinhole collimator was used to generate a beam with diameter of 1 mm. Scattering patterns were recorded on a two-dimensional Siemens X-1000 area detector with a sample-to-detector distance of 130 cm. The experimental conditions for the SAXS measurements were the same for all diffractograms depicted. Three scattering experiments were performed for each shearing condition, corresponding to three orthogonal directions with respect to the deformation geometry as illustrated in the figures. If not stated otherwise, all 2D-SAXS patterns were measured at a point on the samples corresponding to 60% strain.

Orientational order parameters $\langle P_2(\cos \beta) \rangle$ for the lamellar normal \mathbf{n} , a unit vector normal to the lamellar interface, were calculated using a procedure outlined in ref 36. Here, β is the angle between \mathbf{n} and the preferential orientation direction of \mathbf{n} , which is parallel to the velocity gradient direction of the flow field for the parallel orientation and perpendicular to the velocity gradient direction as well as the flow direction for the perpendicular orientation, respectively.

Results and Discussion

As pointed out in the Introduction, it is instructive to examine first the linear viscoelastic properties in order to get a dynamic fingerprint of the block copolymer under study. The frequency dependence of the dynamic shear moduli and shear viscosity of an unoriented sample of PS-PI-7 measured at 409 K, which is 15 K below T_{ODT} , is shown in Figure 1. From the three frequency regimes for the dynamic shear viscosity described in our previous paper,²⁹ only the central frequency regime and the onset of the low-frequency regime are present due to the limited frequency range studied. At the high-frequency end, the viscosity has a moderate slope and the loss modulus G'' is higher than

the storage modulus G' . Viscous contributions dominate the relaxation under shear flow in this frequency regime. As the shear frequency is decreased, the slope of the shear viscosity η' increases. At the same time, the storage modulus increases relative to the loss modulus and dominates the behavior at the low-frequency end. In analogy to the analysis of Koppi et al.²¹ and in our earlier publication,²⁹ we identify the critical frequency ω_d as the point at which the dynamic shear viscosity starts to deviate from the line of constant slope (see Figure 1). Although T_{ODT} is 20 K higher, the similarity of the linear viscoelastic properties between this new sample and the diblock copolymer used in our previous study is quite apparent.

Next, the frequency dependence of orientation of the lamellar microstructure under large-amplitude oscillatory shear flow for these two frequency regimes was investigated. As in our earlier work,²⁹ the samples pressed at room temperature were first annealed under vacuum at 358 K, i.e. roughly 20 K above the T_g of the PS blocks but far below T_{ODT} , for more than 24 h and then cooled slowly to room temperature. After heating to 409 K in the rheometer under nitrogen and temperature equilibration for about 20 min, the samples were oriented under large-amplitude (100% strain) oscillatory shear flow for 10 h with different frequencies within the two frequency regimes described above. The resulting morphologies were then examined using 2D-SAXS measurements.

Two representative 2D-SAXS results of samples oriented with frequencies $\omega_1 = 10$ rad/s and $\omega_2 = 0.1$ rad/s are shown in Figures 2a and 2b, respectively. The first shear frequency $\omega_1 = 10$ rad/s falls in the central frequency regime above ω_d in Figure 1. The 2D-SAXS measurements of the oriented sample show strong scattering peaks along \mathbf{q}_{rad} in both the \mathbf{q}_{nor} - \mathbf{q}_{rad} and the \mathbf{q}_{rad} - \mathbf{q}_{tan} planes, while the scattering in the \mathbf{q}_{nor} - \mathbf{q}_{tan} plane is rather small (Figure 2a). This indicates that the normal unit of the lamellar microstructure is aligned preferentially in the radial direction (\mathbf{q}_{rad}) of the sample disk as schematically indicated on the right-hand side of Figure 2a. This morphology is conventionally termed "perpendicular" orientation. A quantitative analysis of the pattern, corresponding to the tangential view (\mathbf{q}_{nor} - \mathbf{q}_{rad} plane) yields an order parameter $\langle P_2 \rangle$ of 0.58. It reveals a state of order comparable to that typically obtained in the nematic phase of liquid crystals.

The second sample was oriented at a frequency $\omega_2 = 0.1$ rad/s, which falls well into the lower frequency regime shown in Figure 1. The resulting 2D-SAXS diffractograms are distinctly different. Here strong SAXS peaks are found along \mathbf{q}_{nor} in both the \mathbf{q}_{nor} - \mathbf{q}_{tan} and \mathbf{q}_{nor} - \mathbf{q}_{rad} planes, while the scattering in the \mathbf{q}_{rad} - \mathbf{q}_{tan} plane is rather small (Figure 2b). This shows that the normal unit of the lamellar microstructure is oriented parallel to the velocity gradient direction, commonly referred to as the "parallel" orientation, as schematically indicated on the right-hand side of Figure 2b. A quantitative analysis of the pattern, corresponding to the tangential view (\mathbf{q}_{nor} - \mathbf{q}_{rad} plane) yields an order parameter $\langle P_2 \rangle$ of 0.78. It reveals a state of high order comparable to that typically obtained in smectic phases of liquid crystals. In summary, these results confirm the existence of the two lower frequency regimes for the lamellar microstructure orientation under large-amplitude oscillatory shear flow²⁹ which lead to perpendicular and parallel orientation, respectively.

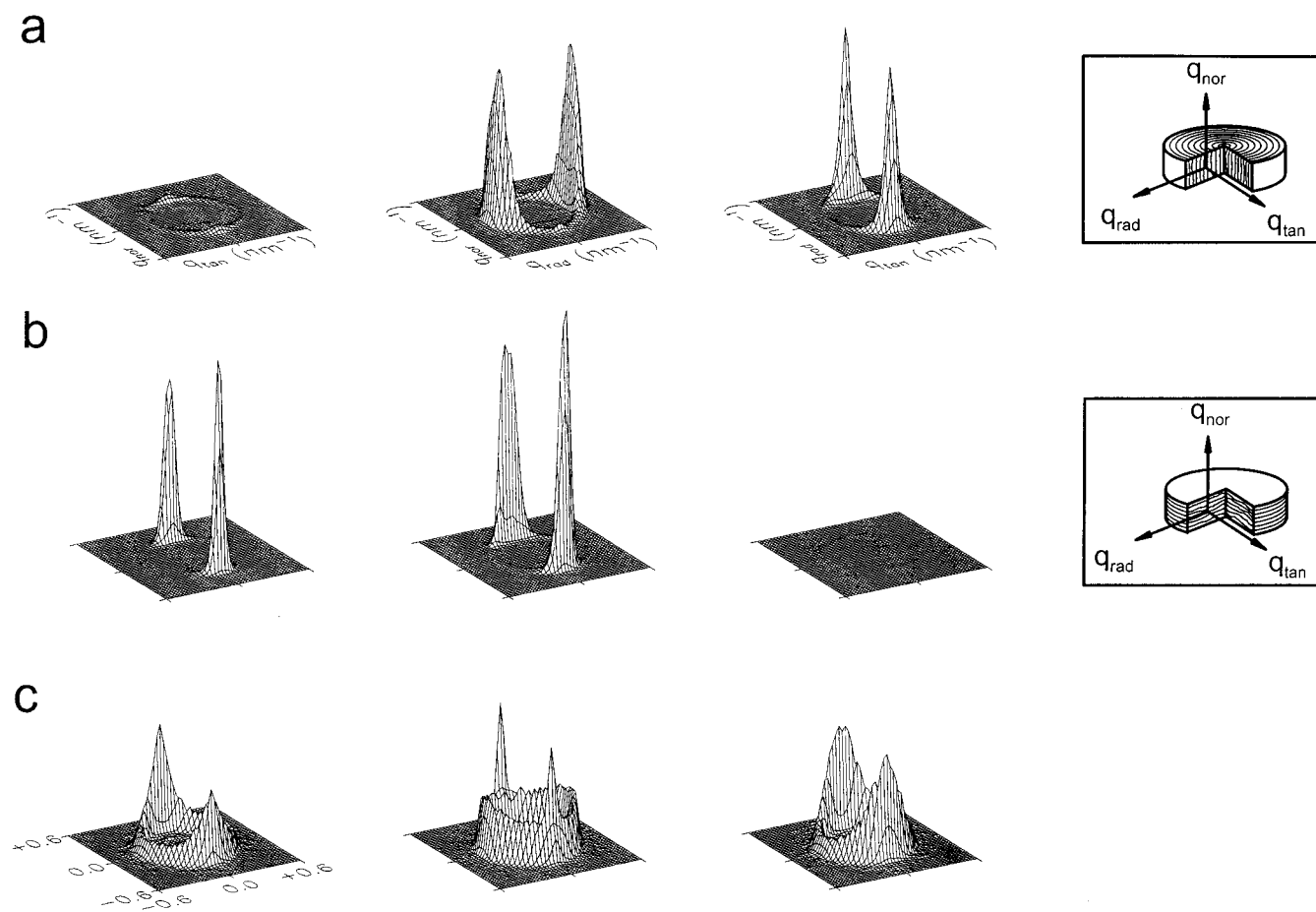


Figure 2. Two-dimensional SAXS results for PS-PI-7 following large-amplitude oscillatory shear (100% strain) for 10 h at 409 K. Specimens were cut and measured at a point which corresponds to 60% strain. Annealed samples (see text for thermal history): (a) $\omega_1 = 10$ rad/s; (b) $\omega_2 = 0.1$ rad/s. Quenched sample (see text for thermal history): (c) $\omega_2 = 0.1$ rad/s. The intensities of the patterns in (a) and (c) are multiplied by a factor of 2.5 and 10, respectively, in order to obtain signal heights comparable to those in (b). In the insets on the right-hand side the resulting orientations are schematically depicted together with the coordinate frame used for the cases of uniform orientation behavior (a) and (b). From left to right the diffractograms correspond to the radial, tangential, and normal view of the sample disks, respectively.

Thermal history has significant effects on many properties of complex polymer systems. In the case of block copolymers, annealing is important due to the presence of imperfections, namely defects and grain boundaries. It is interesting, therefore, to explore the effect of the thermal history of lamellar diblock copolymer samples on their orientation behavior. To this end, some samples thermally treated as described above were not directly heated in the rheometer to the desired shearing temperature but were first taken to 433 K, which is 9 K above T_{ODT} . After 20 min at this temperature, they were quenched to 409 K over 5 min. Then after temperature equilibration for another 20 min, large-amplitude (100% strain) oscillatory shear flow was applied to orient the samples. In the following discussion, samples quenched from 433 K before orientation will be called "quenched". Those samples thermally treated as described above but heated from room temperature directly to 409 K for orientation experiments will be called "annealed" samples. A typical 2D-SAXS result obtained for a quenched sample which was oriented with frequency $\omega_2 = 0.1$ rad/s for 10 h is shown in Figure 2c. Broad SAXS peaks are present in both the \mathbf{q}_{nor} - \mathbf{q}_{tan} and \mathbf{q}_{rad} - \mathbf{q}_{tan} planes along \mathbf{q}_{nor} and \mathbf{q}_{rad} , respectively. For the \mathbf{q}_{nor} - \mathbf{q}_{rad} plane, a mixture of narrow peaks along \mathbf{q}_{nor} and very broad peaks along \mathbf{q}_{rad} is obtained. In addition, the SAXS peaks in Figure 2c are much weaker than those in Figures 2a and 2b. While the intensities of the patterns in Figure 2a are

multiplied by a factor of 2.5, those in Figure 2c are scaled by a factor of 10 in order to obtain signal heights comparable to those of Figure 2b. This can be directly inferred from comparison of the noise around the SAXS peaks. It is quantitatively reflected in order parameters of less than 10% for the quenched sample. All of these features show that in the low-frequency regime, in contrast to the annealed samples, the lamellar microstructure in the quenched sample is not uniformly oriented under shear flow and does not exhibit large order parameters. Since the shear conditions in cases b and c were identical, i.e. equal frequency, strain, and time, we therefore conclude that the thermal history of the lamellar diblock copolymer samples significantly affects their orientation behavior under large-amplitude oscillatory shear flow.

For the annealed samples, the orientation of the lamellar microstructure is independent of shear strain under the two experimental conditions described earlier (above the threshold value for orientation). This was checked by 2D-SAXS measurements along the radial direction of the sample disks (not shown here). In contrast, for all the quenched samples, a large strain and time dependence of orientation is observed. This is demonstrated in Figure 3, showing more 2D-SAXS results measured in the tangential direction, i.e. in the \mathbf{q}_{nor} - \mathbf{q}_{rad} plane of quenched samples. The first 2D-SAXS pattern (Figure 3a) was measured using the same quenched sample disk described above (Figure 2c) that

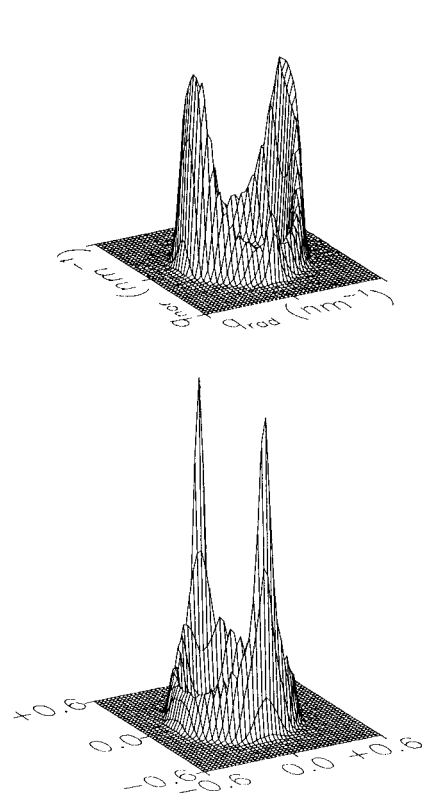


Figure 3. 2D-SAXS results measured in the tangential direction, i.e. the $\mathbf{q}_{\text{nor}}-\mathbf{q}_{\text{rad}}$ plane, for PS-PI-7 following large-amplitude oscillatory shear (100% strain) with frequency $\omega_2 = 0.1$ rad/s at 409 K: (a) quenched sample sheared for 10 h (same sample as in Figure 2c) but cut and measured at a point which corresponds to 90% strain; (b) quenched sample sheared for 20 h and cut and measured at a point corresponding to 60% strain. The intensities of the patterns in (a) and (b) are multiplied by a factor of 6.3 and 4.2, respectively, in order to obtain signal heights comparable to those in Figure 2b. The patterns should be compared with those in the middle column of Figure 2.

was oriented with frequency $\omega_2 = 0.1$ rad/s for 10 h at 409 K. But this time a point corresponding to 90% strain, i.e. further out along the radius, was chosen. For this strain value, the diffractogram is dominated by rather broad peaks along \mathbf{q}_{rad} while only very small and narrow peaks can be detected along \mathbf{q}_{nor} . Note the difference to the middle pattern in Figure 2c. This indicates that for the same shearing time but a larger strain value the lamellar microstructure in the sample is preferentially aligned in the perpendicular direction. The second 2D-SAXS pattern (Figure 3b) was measured at the 60% strain point on a freshly prepared quenched sample which was oriented with frequency $\omega_2 = 0.1$ rad/s as before (Figure 2c) but sheared for 20 h. In contrast to the patterns in Figures 2c and 3a, it presents dominant SAXS peaks along \mathbf{q}_{nor} together with a high isotropic background. This indicates that the parallel orientation dominates in quenched samples for very long shearing times. Thus, for quenched samples, quite different orientation behavior can be obtained in the low-frequency regime as deduced from the shear viscosity measurements (Figure 1) depending on the strain value and shearing time.

To determine the source of thermal history effects, different sample preparation methods were examined. Several samples were annealed at 433 K (above T_{ODT}) for 20 min. Then the first sample was quenched to 409 K and annealed again at that temperature for more than 24 h. The second sample was first quenched to

308 K, i.e. below T_g of the PS blocks. After 40 min at this temperature, it was reheated to 409 K. The third sample was quenched to 358 K, i.e. above T_g of the PS blocks, and annealed at that temperature for more than 24 h. Then all of these samples were sheared with frequency $\omega_2 = 0.1$ rad/s for 10 h at 409 K. The SAXS results of the first two samples are similar to that shown in Figure 2c. Only the third sample presents the same 2D-SAXS patterns as that shown in Figure 2b, i.e. uniform parallel orientation. These observations indicate that the crucial step to obtain uniform orientation behavior exhibiting high order parameters is to anneal the sample at a temperature (358 K in our case) far below T_{ODT} but above the glass transition temperatures of the two blocks, for long enough times before large-amplitude oscillatory shear flow is applied.

Finally, we checked whether annealing at low temperatures induces any changes in the dynamic behavior of the diblock copolymer samples. Linear viscoelastic properties of annealed and quenched samples as obtained from small-strain dynamic mechanical experiments were therefore compared. As expected from studies of temperature jump experiments by other groups,^{35,37-39} no significant differences to account for the thermal history effect on the lamellar orientation behavior were detected. In contrast, the on-line decay curves of dynamic moduli measured during large-amplitude oscillatory shearing show significant and reproducible differences for the annealed and the quenched samples (not shown here). Obviously, annealing far below T_{ODT} but above the glass transition temperatures of both blocks induces changes which leave the linear response of lamellar diblock copolymers essentially unaltered. They seem to substantially influence the nonlinear response, however, leading to different orientation behavior under large-amplitude oscillatory shear flow of annealed and quenched samples.

It is interesting to note that recently Balsara and co-workers have observed that the signatures of the ODT in cylindrical PS-PI block copolymers depend crucially on the coherence length of the ordered structures, which, in turn, is governed by annealing history.⁴⁰ We have previously proposed that in the low-frequency regime of the shear viscosity the interface is the structural element that supports the stress and thus is believed to reorient as a whole under large-amplitude oscillatory shear flow.²⁹ It can therefore be expected that the correlation length of orientation is a critical parameter for the reorientation process of the lamellae. Further studies, however, are necessary to elucidate this point to lead to a better understanding of the molecular origin of the observed behavior.

Conclusions

We have demonstrated that in the low-frequency regime of the dynamic shear viscosity of a lamellar PS-PI diblock copolymer near T_{ODT} the lamellar orientation behavior under large-amplitude oscillatory shear flow is strongly influenced by the thermal history of the sample. For samples annealed at temperatures far below T_{ODT} but above the glass transition temperatures of both blocks, parallel alignment of the unit normal with respect to the velocity gradient direction is reproducibly achieved. For unannealed samples quenched from above T_{ODT} , preferential perpendicular alignment can be generated. Only for annealed samples, however, uniform orientation patterns with optimum order parameters are obtained. These results explain apparent

differences in the orientation behavior at low frequencies for lamellar PS-PI diblock copolymers near T_{ODT} between our and other groups^{26,27,41} since in contrast to our work only quenched samples from above T_{ODT} were employed in these investigations. It is interesting to note that in their paper about the frequency dependence of orientation of PEP-PEE diblock copolymers, Koppi et al. never quenched their samples from above T_{ODT} but rather annealed them at lower temperatures before shearing.²¹ Indeed the orientation patterns obtained by small-angle neutron scattering of their samples are equivalent to ours. Moreover, using this procedure, Wang et al.⁴² recently observed three frequency regimes of orientation for a lamellar polystyrene-polybutadiene diblock copolymer at temperatures close to T_{ODT} , in agreement with our results on PS-PI. From all these observations, we conclude that lamellar diblock copolymers subjected to large-amplitude oscillatory shear flow show a common behavior. So far, no counterexamples have been reported.

Acknowledgment. We thank T. Wagner and T. Volkmer for their help in preparing our samples, T. Hirschmann for his support in performing the mechanical measurements, and M. Bach for the help with the SAXS measurements. Y.Z. thanks the Volkswagen Stiftung for a stipend.

References and Notes

- (1) Keller, A.; Pedemonte, E.; Willmouth, F. M. *Nature* **1970**, *225*, 538.
- (2) Terrisse, J. Ph.D. Thesis, L'Université Louis Pasteur de Strasbourg, Strasbourg, France, 1973.
- (3) Hadzioannou, G.; Mathis, A.; Skoulios, A. *Colloid Polym. Sci.* **1979**, *257*, 136.
- (4) Hadzioannou, G.; Picot, C.; Skoulios, A.; Ionescu, M.-L.; Mathis, S.; Duplessix, R.; Gallot, Y.; Lingelser, J.-P. *Macromolecules* **1982**, *15*, 263.
- (5) Pakula, T.; Saijo, K.; Kawai, H.; Hashimoto, T. *Macromolecules* **1985**, *18*, 1294.
- (6) Morrison, F. A.; Winter, H. H. *Macromolecules* **1989**, *22*, 3533.
- (7) Morrison, F. A.; Winter, H. H.; Gronski, W.; Barnes, J. D. *Macromolecules* **1990**, *23*, 4200.
- (8) Scott, D. B.; Waddon, A. J.; Lin, Y.-G.; Karasz, F. E.; Winter, H. H. *Macromolecules* **1992**, *25*, 4175.
- (9) Ramon, J.; Thomas, E. L. *J. Polym. Sci., Polym. Phys.* **1993**, *31*, 37.
- (10) Almdal, K.; Koppi, K. A.; Bates, F. S. *Macromolecules* **1993**, *26*, 4058.
- (11) Morrison, F. A.; Mays, J. W.; Muthukumar, M.; Nakatani, A. I.; Hahn, C. C. *Macromolecules* **1993**, *26*, 5271.
- (12) Winter, H. H.; Scott, D. B.; Gronski, W.; Okamoto, S.; Hashimoto, T. *Macromolecules* **1993**, *26*, 7236.
- (13) Koppi, K. A.; Tirrell, M.; Bates, F. S. *Phys. Rev. Lett.* **1993**, *70*, 1449.
- (14) Okamoto, S.; Saijo, K.; Hashimoto, T. *Macromolecules* **1994**, *27*, 3753.
- (15) Balsara, N. P.; Dai, H. J.; Kesani, P. K.; Garetz, B. A.; Hammouda, B. *Macromolecules* **1995**, *27*, 7406.
- (16) Kofinas, P.; Cohen, R. E. *Macromolecules* **1995**, *28*, 336.
- (17) Jackson, C. L.; Barnes, K. A.; Morrison, F. A.; Mays, J. W.; Nakatani, A. I.; Han, C. C. *Macromolecules* **1995**, *28*, 713.
- (18) Tepe, T.; Schulz, M. F.; Zhao, J.; Tirrell, M.; Bates, F. S. *Macromolecules* **1995**, *28*, 3008.
- (19) de Gennes, P.-G. *Rev. Mod. Phys.* **1992**, *64*, 645.
- (20) Cross, M.; Hohenberg, P. *Rev. Mod. Phys.* **1993**, *65*, 851.
- (21) Koppi, K. A.; Tirrell, M.; Bates, F. S.; Almdal, K.; Colby, R. H. *J. Phys. II* **1992**, *2*, 1941.
- (22) Winey, K. I.; Patel, S. S.; Larson, R. G.; Watanabe, H. *Macromolecules* **1993**, *26*, 2542.
- (23) Winey, K. I.; Patel, S. S.; Larson, R. G.; Watanabe, H. *Macromolecules* **1993**, *26*, 4373.
- (24) Kannan, R. M.; Kornfield, J. A. *Macromolecules* **1994**, *27*, 1177.
- (25) Okamoto, S.; Saijo, K.; Hashimoto, T. *Macromolecules* **1994**, *27*, 5547.
- (26) Patel, S. S.; Larson, R. G.; Winey, K. I.; Watanabe, H. *Macromolecules* **1995**, *28*, 4313.
- (27) Gupta, V. K.; Krishnamoorti, R.; Kornfield, J. A.; Smith, S. D. *Macromolecules* **1995**, *28*, 4464.
- (28) Riise, B. L.; Fredrickson, G. H.; Larson, R. G.; Pearson, D. S. *Macromolecules* **1995**, *28*, 7653.
- (29) Zhang, Y.; Wiesner, U.; Spiess, H. W. *Macromolecules* **1995**, *28*, 778.
- (30) Zhang, Y.; Wiesner, U. *J. Chem. Phys.* **1995**, *103*, 4784.
- (31) Denault, J.; Morère-Séguéla, B.; Prud'homme, J. *Macromolecules* **1990**, *23*, 4658.
- (32) Schmidt-Rohr, K.; Clauss, J.; Spiess, H. W. *Macromolecules* **1992**, *25*, 3273.
- (33) Cai, W. Z.; Schmidt-Rohr, K.; Egger, N.; Gerharz, B.; Spiess, H. W. *Polymer* **1993**, *34*, 267.
- (34) Rosedale, J. H.; Bates, F. S. *Macromolecules* **1990**, *23*, 2329.
- (35) Stühn, B.; Mutter, R.; Albrecht, T. *Europhys. Lett.* **1992**, *18*, 427.
- (36) Ehlich, D.; Takenaka, M.; Okamoto, S.; Hashimoto, T. *Macromolecules* **1993**, *26*, 189.
- (37) Hashimoto, T.; Sakamoto, N. *Macromolecules* **1995**, *28*, 4779.
- (38) Floudas, G.; Pakula, T.; Fischer, E. W.; Hadjichristidis, N.; Pispas, S. *Acta Polym.* **1994**, *45*, 176.
- (39) Stühn, B.; Vilesov, A.; Zachmann, H. G. *Macromolecules* **1994**, *27*, 3560.
- (40) Perahia, D.; Vacca, G.; Patel, S. S.; Dai, H. J.; Balsara, N. P. *Macromolecules* **1994**, *27*, 7645.
- (41) Gupta, V. K.; Krishnamoorti, R.; Chen, Z.-R.; Kornfield, J. A.; Smith, S. D.; Satkowski, M. M.; Grothaus, J. T. *Macromolecules* **1996**, *29*, 875.
- (42) Wang, S.; Deodorigo, W.; Stamm, M.; Pakula, T., in preparation.

MA9601631